Identification, Purification, and Molecular Cloning of N-1-Naphthylphthalmic Acid-Binding Plasma Membrane-Associated Aminopeptidases from Arabidopsis[1]

Angus S. Murphy*, Karen R. Hoogner, Wendy Ann Peer, and Lincoln Taiz

Department of Horticulture and Landscape Architecture, Purdue University, West Lafayette, Indiana 47907–1165 (A.S.M., W.A.P.); and Molecular, Cellular and Developmental Biology Department, University of California, Santa Cruz, California 95064 (K.R.H., L.T.)

Polar transport of the plant hormone auxin is regulated at the cellular level by inhibition of efflux from a plasma membrane (PM) carrier. Binding of the auxin transport inhibitor N-1-naphthylphthalamic acid (NPA) to a regulatory site associated with the carrier has been characterized, but the NPA-binding protein(s) have not been identified. Experimental disparities between levels of high-affinity NPA binding and auxin transport inhibition can be explained by the presence of a low-affinity binding site and in vivo hydrolysis of NPA. In Arabidopsis, colocalization of NPA amidase and aminopeptidase (AP) activities, inhibition of auxin transport by artificial β-naphthylamide substrates, and saturable displacement of NPA by the AP inhibitor bestatin suggest that PM APs may be involved in both low-affinity NPA binding and hydrolysis. We report the purification and molecular cloning of NPA-binding PM APs and associated proteins from Arabidopsis. This is the first report of PM APs in plants. PM proteins were purified by gel permeation, anion exchange, and NPA affinity chromatography monitored for tyrosine-AP activity. Lower affinity fractions contained two orthologs of mammalian APs involved in signal transduction and cell surface-extracellular matrix interactions. AtAPM1 and ATAPP1 have substrate specificities and inhibitor sensitivities similar to their mammalian orthologs, and have temporal and spatial expression patterns consistent with previous in planta histochemical data. Copurifying proteins suggest that the APs interact with secreted cell surface and cell wall proline-rich proteins. AtAPM1 and AtAPP1 are encoded by single genes. In vitro translation products of *ATAPM1 and AtAPP1* have enzymatic activities similar to those of native proteins.

Auxin is an essential multifunctional plant hormone that induces cell elongation and root branching, determines polarity in developing embryos, and shapes plant form during normal and tropic growth. Indole acetic acid, the most common auxin, is synthesized in the growing apical shoot region and is transported basipetally by a chemiosmotic polar transport mechanism that is regulated at the cellular level. The auxin transport inhibitor N-1-naphthylphthalamic acid (NPA) has a long history as a valuable tool in the study of auxin transport in a variety of plant species (Rubery, 1990). Although the exact mechanism by which NPA inhibits polar auxin transport is unknown, biochemical studies indicate that NPA interferes with the cellular efflux of auxin from anion channels by binding to a distinct regulatory site rather than the auxin channel pore itself (Muday, 2001). The recent cloning of the PIN genes that encode a putative auxin efflux carrier in Arabidopsis (Chen et al., 1998; Gälweiler et al., 1998; Luschnig et al., 1998; Müller et al., 1998; Utsuno et al., 1998) has refocused attention on the mechanisms that regulate polar auxin transport and the proteins with which NPA interacts.

Although NPA-binding proteins have been localized to the plasma membrane (PM) in all plant species studied to date (Lomax et al., 1995) and can be found in virtually all tissues (Katekar and Geissler, 1989), they have proven to be difficult to purify to homogeneity. A single flavonoid-sensitive, high-affinity NPA-binding site that is associated with both a peripheral membrane F-actin-binding protein and an integral membrane protein has been extensively characterized in zucchini (*Cucurbita pepo*) hypocotyls (for review, see Muday, 2001). Biochemical evidence suggests that a similar NPA-binding protein exists in other tissues and plant species. However, the light dependence of NPA-induced growth inhibition in some tissues and not others (Geissler et al., 1985; Jensen et al., 1998) suggests that more than one NPA-sensitive regulatory protein or protein complex may be present. This possibility is further suggested both by a disparity between NPA binding and auxin transport inhibition (Katekar et al., 1987) and the association of auxin transport inhibition with a separate, low-affinity NPA-binding site in zucchini (Michalke et al., 1992). As NPA is hydrolyzed in planta and non-hydrolyzable NPA analogs are better inhibitors of auxin transport than NPA (Katekar et al., 1987), it has been suggested that a PM-associated amidase

[1] This work was supported by the U.S. Department of Agriculture (grant no. 94–37100–0755).

* Corresponding author; e-mail amurphy@hort.purdue.edu; fax 765–494–0391.

Article, publication date, and citation information can be found at www.plantphysiol.org/cgi/doi/10.1104/pp.010519.

might account for both weak NPA binding and the disparity between NPA binding and activity profiles.

Recently, we identified a low-affinity, flavonoid-sensitive NPA amidase activity in Arabidopsis and showed that it colocalized both spatially and temporally with PM aminopeptidase (AP) activity, auxin accumulation, and aglycone flavonoid production (Murphy and Taiz, 1999a, 1999b; Murphy et al., 2000; Peer et al., 2001). The possibility that the observed PM APs might be responsible for both weak NPA binding and hydrolysis was reinforced when both artificial Tyr-, Pro-, Gly-Pro-, and Trp-AP substrates and the specific AP inhibitor bestatin were shown to inhibit polar auxin transport. The same compounds also displaced NPA in a saturable manner from a low-affinity binding site in Arabidopsis microsomal vesicles. These results suggested not only a potential mechanism for low-affinity NPA binding and hydrolysis, but also provided a strategy for purifying components of the NPA-sensitive auxin transport regulatory apparatus.

In this paper, we describe the purification, characterization, and molecular cloning of two NPA-binding PM APs from Arabidopsis that represent two classes of APs never identified before in plants. These novel PM APs are orthologs of mammalian proteins that participate in cell surface signal transduction by processing the neuropeptides kyotorphin and Met-enkephalin (Akasaki et al., 1995), the secretory inhibitor PYY (Medeiros and Turner, 1994), the vasodilator bradykinin (Venema et al., 1997), dynorphin (Nissen et al., 1995), and other cell surface signaling components (Santos et al., 2000). Mammalian PM APs of these types also process secreted cell surface and ECM components in the trans-Golgi (Foulon et al., 1999), participate in vesicular cycling of asymmetrically distributed transporters (Baumann and Saltiel, 2001), and remodel ECM components at the cell surface (Dean and Sansom, 2000). Like their orthologs in Arabidopsis, mammalian PM APs show little affinity for the Leu substrates most preferred by the Leu APs associated with protein turnover and mobilization in animals and plants (Taylor, 1996; Walling and Gu, 1996). The conclusive identification of the plant PM APs described herein adds to the growing evidence that cellular interactions with the ECM and extracellular peptides are as significant in plant growth and development as in animals.

RESULTS

Purification of NPA-Binding Proteins in Fractions with Tyr-AP Activity

In previous work, we have shown that Tyr-AP activity consistently co-occurred with NPA amidase activity, especially in purified PM vesicles. It is important that PM Tyr-AP activity is only slightly phenylmethane fluorosulfonate (PMSF) sensitive (Murphy and Taiz, 1999b), whereas crude microsomal vesicles contain high levels of PMSF-sensitive Tyr-AP and Leu-AP activity (data not shown). Therefore, as a precaution against enrichment for non-PM contaminants, only fractions containing PMSF-insensitive Tyr-AP activity > Leu-AP acitivity were selected at each purification step.

PM proteins from 5-d-old Arabidopsis seedlings were assayed for purity as previously described (Murphy and Taiz, 1999a), detergent solubilized under non-denaturing conditions, and purified by gel permeation and anion-exchange chromatography. Although NPA binding to the high-affinity binding site requires a free carboxylic acid on the phthalic acid moiety (Katekar et al., 1987), we reasoned that lower affinity binding suitable for chromatography would be possible if NPA was immobilized by conjugation with an amine-terminated spacer arm of the correct length and utilized under conditions in which the linkage would best mimic a free carboxylic acid. The affinity substrate synthesis and experimental conditions described (see "Materials and Methods") were the only conditions under which reproducible specific binding and separation could be achieved in our hands. The proteins retained on NPA-conjugated beads were washed with 50 mM KCl to eliminate nonspecific binding, then eluted with 350 mM KCl. No Tyr-AP activity was detected in 50 mM washes. Fractions containing PMSF-insensitive Tyr-AP activity from each purification step were analyzed by SDS-PAGE (Fig. 1A).

Proteins eluted from NPA-conjugated beads as above were then analyzed for Tyr-AP activity after native gel electrophoresis using Tyr-AFC enzyme overlay membranes to visualize AP activity (see "Materials and Methods"). Two distinct groups of proteins with Tyr-AP activity were visible when Tyr-AFC enzyme overlays were visualized under near UV light (Fig. 1B).

Because APs are generally glycoproteins (Taylor, 1996), proteins eluted from NPA-conjugated beads were separated by SDS-PAGE and then stained with PAS to detect glycoproteins. As shown in Figure 1C, four groups of diffuse bands indicated the presence of glycoproteins. Analysis of SDS-PAGE band shifts after enzymatic or chemical deglycosylation indicated that at least 10 glycoproteins were present in this fraction (data not shown).

To achieve further separation, NPA-bound PM proteins were eluted with a linear KCl gradient (50–350 mM). Dialyzed fractions were than analyzed for Tyr-AP activity. As shown in Figure 1D, approximately 90% of detected Tyr-AP activity was found in fractions corresponding to protein peak II (100–160 mM KCl). This result is consistent with earlier studies indicating that PM AP activities were associated with low rather than high-affinity NPA-binding fractions (Murphy et al., 2000). The complex nature of the Tyr-AP activity profile associated with peak II is also

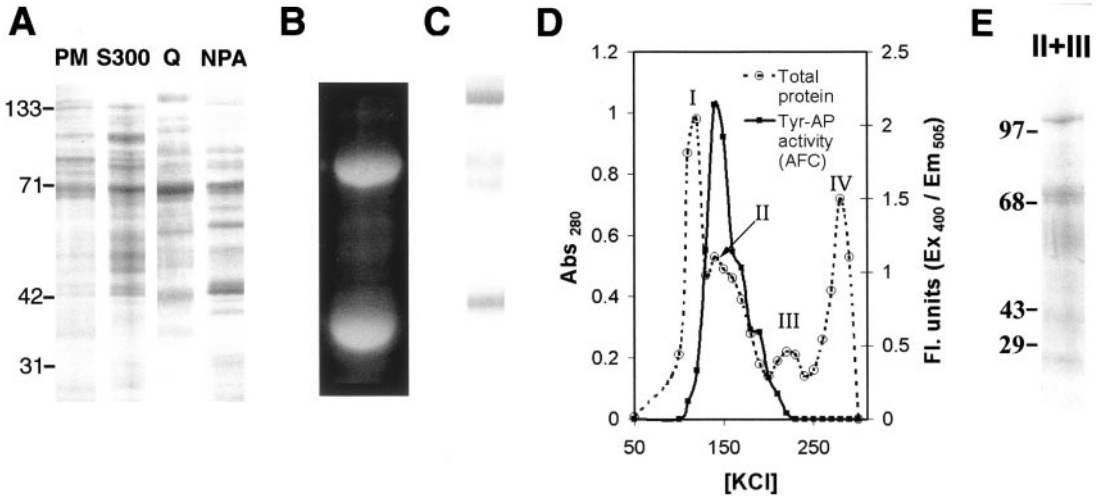

Figure 1. Purification of NPA-binding proteins with Tyr-AP activity from Arabidopsis PM vesicles. A, Silver stained SDS-PAGE gels of Tyr-AP peak fractions (1 μg of total protein per lane) from each purification stage. PM, Solubilized PM vesicle proteins; S300, Sephacryl S300 gel permeation chromatography peak fraction; Q, Q resin anion-exchange peak fraction; NPA, NPA affinity fraction (350 mM KCl). B, Tyr-aminofluoromethylcoumarin (AFC) enzyme overlay visualization of AP activity of NPA-binding proteins analyzed by native PAGE. C, Periodic acid-Schiff's reagent (PAS) staining of NPA-binding glycoproteins. D, Elution profiles (50–300 mM KCl) of proteins from NPA affinity beads. Dotted line, A_{280}; solid line, Tyr-AP activity assayed fluorometrically with Tyr-AFC substrate. Protein peak fractions identified with Roman numerals. E, Silver-stained 4% to 20% (w/v) SDS-PAGE gel of combined NPA affinity fractions II and III (100 ng of total protein).

consistent with the two separate proteins or protein complexes shown in Figure 1B.

Characterization of PM AP Activities

In previous studies of whole PMs from Arabidopsis seedlings, four AP activities colocalized with NPA amidase activity: Tyr-, Pro-, X-Pro-, and Trp-AP (Murphy and Taiz, 1999a, 1999b; Murphy et al., 2000). To determine if purified PM NPA-binding proteins had the same AP activities as whole PM vesicles, the amidase activity of the fractions that had been selected after each stage of the purification process were assayed with AP substrates and NPA itself. As shown in Table I, after detergent solubilization, all AP- and NPA amidase-specific activities decreased, presumably because of a loss of membrane interactions with either the enzymes themselves, other proteins, or native cofactors. Subsequently, however, fractions from S300 gel permeation and anion (Q-resin) exchange chromatography all showed enrichment of NPA amidase and Tyr-, Ala-Pro- (X-Pro), and Pro-specific activities. The observed decrease of Leu- and Trp-AP-specific activities to levels near the limit of detection could not have been predicted from previous whole PM studies.

When NPA-affinity chromatography fractions were assayed, AP and NPA amidase activities were detected in fraction II and, to a lesser extent, fraction III, but not in fractions I and IV (Table I). Specific activities of peak III fractions ranged from 2% (X-Pro-AP) to 55% (Ala-AP) of peak II activities. When com-

Table I. *Specific AP and NPA amidase activities of PM proteins at each step of purification*

Fractions (100 ng) from each purification step were assayed for activity after dialysis against AP assay buffer for 1 h at 4°C. AFC conjugate concentrations were 20 μM. Ala-β-naphthylamide (NA) and NPA concentrations were 100 μM. PM, PM-enriched membranes; Solubilized, detergent-solubilized PM proteins; S300, Sephacryl S-300 PMSF-insensitive peak fraction; Q resin, Q anion-exchange PMSF-insensitive peak fraction; NPA peaks I through III, fractions (or combinations of fractions) corresponding to NPA affinity A_{280} peaks (Fig. 1D). All assays were repeated at least three times with similar results.

Substrate	PM	Solubilized	S300	Q Resin	NPA Peak II	NPA Peak III	NPA Peak II + III
				nmol min^{-1} mg^{-1}			
Tyr-AFC	31.6	16.6	78.1	226.8	59.3	7.7	392.4
Ala-Pro-AFC	17.6	13.5	15.7	22.4	89.5	1.9	66.3
Trp-AFC	20.2	17.1	3.3	4.7	2.2	1.7	4.7
Pro-AFC	16.7	15.6	27.9	31.5	27.1	5.9	46.1
Ala-AFC	2.6	2.4	16.1	62.8	27.2	7.5	84.6
Leu-AFC	10.3	9.4	18.2	19.7	2.5	3.1	2.1
Ala-NA	2.1	1.6	2.7	31.6	32.1	18.4	45.7
NPA	6.3	4.4	5.8	25.1	17.1	9.5	42.1

pared with the Tyr-AP-specific activity of anion-exchange peak fractions (Table I, Q resin), the Tyr-AP activity of NPA affinity fraction II was dramatically reduced. To determine whether the proteins contained in other affinity fractions interacted synergistically to enhance the Tyr-AP activity in fraction II, fractions II and III were reconstituted and reanalyzed. As shown in the last column of Table I, the specific Tyr-AP activity of fractions II and III combined was nearly 2 times the specific activity of fractions corresponding to the anion-exchange Tyr-AP peak. Ala-AP- and NPA amidase-specific activities increased 1.3 and 1.6 times, respectively, in the reconstituted fractions. Reconstitution of fraction II with either affinity fraction I or IV resulted in no increase in activity (data not shown). The components of the combined affinity fractions II and III, analyzed by SDS-PAGE, are shown in Figure 1E. Taken together with the results from AP enzyme overlay analysis of native gels (Fig. 1B) and earlier partitioning studies of peripheral-integral PM NPA activity (Murphy and Taiz, 1999a), these results again suggested that at least two proteins or protein complexes with amidase activity were present.

Inhibitor Studies of NPA-Binding APs

To further determine what type of enzymes might be responsible for the AP activities detected, the Tyr, Ala, Ala-Pro, and Pro-AP activities of the reconstituted NPA-binding fractions described above were further characterized in the presence of inhibitors of specific classes of proteases (Table II). The inhibitors assayed were: (a) NPA; (b) EGTA, an inhibitor of metallopeptidases; (c) PMSF, an inhibitor of Ser proteases and some dipeptidyl APs; (d) bestatin, an inhibitor of Leu APs; (e) amastatin, an inhibitor of microsomal (M-type) APs; (f) apstatin, an inhibitor of membrane-associated X-Pro/neutral (P-type) APs; (g) puromycin, an inhibitor of some P- and M-type APs; (h) PAQ22, a newly developed phthalimide inhibitor of mammalian microsomal APs that is structurally similar to NPA (Komoda et al., 2001); (i) DTT, a thiol reductant inhibitor of some dipeptidyl APs; (j) vanadate, an inhibitor of ATP-dependent bacterial amidases; and (k) thiorphan, an inhibitor of neutral metallo-endopeptidases.

Consistent with the presence of a mixture of microsomal metallo-aminopeptidase M (AP-M, EC 3.4.11.2) and a metal-activated X-Pro/neutral aminopeptidase (AP-P, EC 3.4.11.9) in peaks II and III, Tyr-AP activity was sensitive to bestatin, PAQ22, apstatin, EGTA ($P < 0.01$), and, to a lesser extent, puromycin ($P < 0.01$) and amastatin ($P < 0.05$). Ala-AP activity, which is characteristic of microsomal AP-M and not AP-P, was strongly inhibited by AP-M inhibitors EGTA, PAQ22, bestatin, amastatin, and puromycin ($P < 0.01$). Consistent with the presence of a P-type AP (AP-P), Ala-Pro (X-Pro) AP activity was strongly inhibited by apstatin and the reductant DTT ($P < 0.01$), but was also inhibited to a lesser extent by PMSF, EGTA, and bestatin ($P < 0.05$). Pro-AP sensitivity to all inhibitors except PAQ22, amastatin, vanadate, and thiorphan ($P < 0.05$) is also consistent with AP-P activity. All activities, particularly Ala-AP, were more sensitive to 50 μM NPA than PM vesicles (Murphy and Taiz, 1999b). Taken together, these results suggested the presence of functional homologs of aminopeptidase M and aminopeptidase P proteins.

Assays of NPA Affinity Fractions for Flavonoid Binding

We previously showed that the NPA-associated AP activity was flavonoid sensitive and that NPA binding to microsomal vesicles from Arabidopsis is inhibited by the aglycone flavonoids kaempferol and quercetin (Murphy and Taiz, 1999a, 1999b; Murphy et al., 2000). A flavonoid-binding assay based on detection with the reagent diphenyl boronic acid (DPBA) was utilized to assay binding of the flavonoids kaempferol and quercetin to NPA affinity fractions. As shown in Figure 2, flavonoid binding was found in all fractions, but flavonoid binding did not correlate strictly with NPA affinity. Although the highest specific binding was found in the fractions containing proteins with the greatest NPA affinity (peak IV), specific flavonoid binding was higher in fraction II than fraction III.

Table II. *Effects of inhibitors on AP activities of PM NPA-binding proteins*

Proteins from NPA affinity fractions II and III (Fig. 1D) were reconstituted by dialysis in AP assay buffer, then assayed fluorometrically for AP activity with AFC conjugates (20 μM) in the presence or absence of inhibitors. Values shown for inhibitor assays are percent control-specific activities (SA). Values calculated are derived from means and SD of three independent experiments. Table entries marked with an asterisk were significantly different from their control ($P < 0.05$) when analyzed by Student-Newman-Keuls ANOVA.

Substrate	Control SA	NPA (50 μM)	EGTA (2 mM)	PMSF (100 μM)	Bestatin (20 μM)	Amastatin (20 μM)	Apstatin (20 μM)	Puromycin (20 μM)	PAQ22 (20 μM)	Dithiothreitol (DTT; 5 mM)	Vanadate (5 mM)	Thiorphan (50 μM)
	nmol min^{-1} mg^{-1}						%					
Tyr-AFC	381 ± 17.5	65	58	78	41	72	53	61	48	108	95	101
Ala-Pro-AFC	71 ± 7.7	76	84	71	84	87	26	87	98	69	93	97
Ala-AFC	89 ± 5.3	54	20	87	36	37	94	53	34	96	97	98
Pro-AFC	44 ± 9.2	81	79	79	58	88	61	66	99	73	90	97

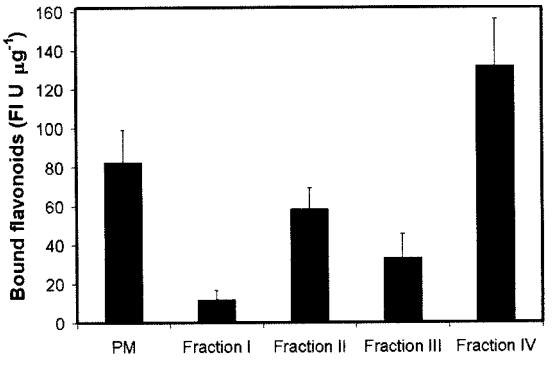

Figure 2. Flavonoid binding of NPA affinity chromatography peak fractions (Fig. 1D). Aglycone flavonoid binding of solubilized PM and NPA affinity fraction proteins was detected fluorometrically with DPBA. Values shown are means and SD of three independent experiments.

Amino Acid Sequencing of NPA-Binding APs

Proteins from NPA affinity fractions I through IV were separated by two-dimensional gel electrophoresis or C8 reverse phase HPLC. Amino acid sequences of internal fragments were obtained as described (see "Materials and Methods"). The amino acid sequences obtained were compared with the National Center for Biotechnology Information (NCBI) database. In cases where equivocal matches with cDNA or predicted protein sequences were found, additional internal sequences were generated until a unique match could be made. Unique oligonucleotide primers for each sequence were designed and used to obtain a cDNA product by reverse transcriptase (RT)-PCR. Nucleotide sequences of cDNAs were obtained and confirmed by comparison with published genomic and expressed sequence tag databases. Names of previously unpublished proteins were assigned based on homology and function in cases where experimental evidence was obtained.

Fractions I and IV

Three proteins, AtPGP1 (Sidler et al., 1998; GenBank accession no. CAA43646), AtPGP2 (GenBank accession no. AtPGP2), and AtMDR1 (GenBank accession no. CAA43646), which are *p*-glycoprotein orthologs of animal multidrug resistance proteins, and a trace amount of a cyclophilin 5 homolog (GenBank accession no. CAC00654) were identified as the components of the highest affinity NPA-binding fraction (fraction IV). These proteins and the genes that encode them are described in detail in another paper (Noh et al., 2001). Fraction I contained five secretory proteins, β-adaptin (GenBank accession no. 7484822), the dynamin-like protein ADL1A (Kang et al., 2001; GenBank accession no. P42697), AtSec14p (Jouannic et al., 1998; GenBank accession no. AAG51793), protein disulfide isomerase (GenBank accession no. AAD41430), and an Hsp70 (GenBank accession no. P22953). Because the components of fractions I and IV appeared to have no direct or synergistic AP activities, they are not described in detail.

Fractions II and III

APs

The composition of NPA affinity fractions II and III are summarized in Table III. As predicted by AP substrate/inhibitor studies, NPA affinity fractions II and III contained proteins with a high degree of homology to mammalian APs. Fraction II, which had the highest AP activity, contained two AP-like proteins: (a) FII70 (AtAPP1), a highly conserved ortholog of human (*Homo sapiens*) aminopeptidase P1 (APP1), an X-Pro and neutral amino acid AP (EC 3.4.11.9) found in both membrane and cytosolic fractions of a variety of human tissues; and (b) FII103 (AtAPM1), an ortholog of the mouse (*Mus musculus*) microsomal AP (EC 3.4.11.2), an Ala/neutral amino acid AP homolog of the mammalian insulin-responsive AP (IRAP) involved in processing of secreted proteins and signal peptides. In addition, NPA affinity fraction III contained FIII42 (AtAPM1Δ), which appears to be a processed or degraded product of FII103 (AtAPM1) that retains the conserved AP catalytic site. The amino acid sequences of AtAPP1 and AtAPM1 aligned with their closest homologs (in both cases from mammals) are shown in Figure 3. The predicted catalytic site motifs of each AP are 100% conserved with the mammalian consensus sequence.

Consistent with predicted sequences, both APs are glycosylated. AtAPM1 stains heavily with PAS and is predicted to have multiple glycosylation sites (Fig. 3A). AtAPP1 stained lightly with PAS, which is consistent with the one glycosylation site predicted by PROSITE scan (Fig. 3B), but was also present in a non-glycosylated form (not shown).

AtAPM1 is predicted to be an integral PM protein of the peptidase M1 family with one highly conserved transmembrane domain (residues 193–215), an amino terminal region exposed to the cytosol, and a conserved metallo-AP site (Fig. 3A) in the extracellular domain closest to the membrane surface. AtAPM1 is predicted to have a long extracellular carboxy-terminal tail with no strong homology to any known protein. However, amino acid sequencing (Table III) and immunochemical data (see below) indicate that the predominant form of AtAPM1 on the PM is the truncated protein (AtAPM1Δ).

AtAPP1 is predicted to be a cytosolic protein of the peptidase M24 family, but has two hydrophobic surface regions consistent with a peripheral membrane protein. Both APs contain conserved catalytic domains (Fig. 3, A and B) consistent with their experimentally observed activities. However, an aromatic binding domain proximal to the catalytic site of AtAPM1 (residues 215–228) is consistent with an increased affinity for Tyr-AP substrates.

Table III. *Identification of PM AP-associated proteins purified by NPA affinity chromatography*

Amino acid sequences of tryptic fragments from PM proteins contained in NPA affinity peaks II and III were obtained as described (see "Materials and Methods"). Protein identifications were assigned by NPA affinity fraction (FII or FIII) and SDS-PAGE apparent molecular mass. GenBank protein identification nos. were assigned if there was a unique database match with a similar predicted molecular mass. GP, Glycoprotein; GPI, glycosyl-phosphatidylinositol anchor; E, experimental evidence; P, predicted. K or R, Inferred lysine or arginine residues.

Purified Protein	Post-translational Modifications	Internal Fragment Sequenced	GenBank Protein Identification No.	Amino Acids (Predicted)	Characterized Ortholog	Similarity
						%
Aminopeptidases						
FII-103 (AtAPM1)	GP (E,P)	(K)TLEVPTDLVALSN	CAB36783	879	PS aminopeptidase M (mouse)/IRAP	53
FII-70 (AtAPP1)	GP (E,P)	(K)VSDEANSYFNGLG	CAB16823	634	Aminopeptidase P1 (human)	60
FIII-42 (AtAPM1Δ)	GP (E,P)	(R)VATVVAHELAHQWF	CAB36783	Unknown	Truncated form of AtAPM1	~68
AP-associated proteins						
FIII-68 (AtMyA1)	GP (P)	(R)SVFASAALGK	AAB63637	619	Myrosinase-associated protein (*Brassica napus*)	62
FII-55 (AtHSP70p)	GP (E,P)	(K)DVLK-(R)LVEHFAADEFNK	CAB10440	484	HSP70 (Arabidopsis)	~68
FII-44/66 (AtFAGP2)	GPI; GP (E,P)	(K)AFSDILKSTGADK	CAB40990	403	Fasciclin-like arabinogalactan protein 2 (Arabidopsis)	59
FIII-40 (ATAPL1)	GP (E,P)	(K)LFVFGDSYADTGNI	CAB82926	359	Anther-specific Pro-rich protein (Arabidopsis)	46
FIII-24 (AtGSTF2)	GP (P)	(K)NISQYAIMAIQ	P46422	212	Auxin-binding GST II (Arabidopsis)	100

AP-Associated Proteins

Two putative membrane surface proteins copurified with AtAPM1 and AtAPP1 in NPA affinity fraction II. FII55 (AtHSP70p) is an ortholog of mammalian PM Hsp70 proteins (Ponomarev et al., 2000). AtHSP70p has no predicted endoplasmic reticulum retention signal and is predicted by PROSITE scan to contain extracellular or cell surface motifs. AtHSP70p is predicted by PSORT to be an extracellular protein with a certainty of 82%. FII44/66 (AtFAGP2) is a GPI-anchored arabinogalactan protein with domains homologous with mammalian extracellular fasciclin cell adhesion proteins (Schultz et al., 2000). The designation FII44/66 reflects the 22-kD shift of apparent molecular mass on SDS gels after chemical deglycosylation of the 66-kD native glycoprotein.

Two other putative membrane surface proteins were found in Fraction III. FIII68 (AtMyA1) is a paralog of jasmonate-inducible myrosinase associated proteins found in *B. napus* (Taipalensuu et al., 1997). AtMyA1 contains two amino terminal Jacalin lectin domains usually associated with carbohydrate interactions (Sankarnarayan et al., 1996), four Kelch domains of the type found in F-actin-binding proteins like ENC-1 (Zhao et al., 2000), and a carboxy-terminal Rab9 domain associated with proteins secreted by the trans Golgi network in mammals (Diaz et al., 1997). AtMyA1 is also abundant in Arabidopsis endomembrane fractions (Prime et al., 2000). FIII40 (AtAPL1-*Ath* anther protein-like) is a putative extracellular Pro-rich protein (PRP) with homology to an anther-specific PRP. Both AtAPL1 and AtMyA1 contain motifs consistent with a hydrolase or esterase function. Fraction III also contained the auxin-binding glutathione *S*-transferase AtGSTF2 previously shown by Zettl et al. (1994) to bind NPA with low affinity. AtGSTF2 expressed in *Escherichia coli* has no detectable AP activity (A.S. Murphy, unpublished results). Extensive characterization of AtGSTF2 expression and activity will be published separately.

Determination of Gene Copy Number of *AtAPM* and *AtAPP*

Southern blotting with full-length *AtAPM1* and *AtAPP1* cDNA probes (not shown) and searches of the Arabidopsis genomic sequence database indicate that *AtAPM1*and *AtAPP1* are single genes located on chromosome IV (GenBank accession nos. AL161582.2, AL035525.1, Z99708.1, and AL161590, respectively). Lower stringency Southern blots with AtAPP1 cDNA probes suggested the presence of a second homologous sequence. Subsequent searches of the NCBI database located a gene (hereafter referred to as *AtAPP2*) on chromosome III (accession nos. AC009177.7 and AC009606.4) with a region of homology to both *AtAPP1* and human *APP2* (protein identification no. g11066157). However, no evidence of the presence of an mRNA transcript of *AtAPP2* could be obtained by RT-PCR of total RNA derived from a variety of tissues, developmental stages, and

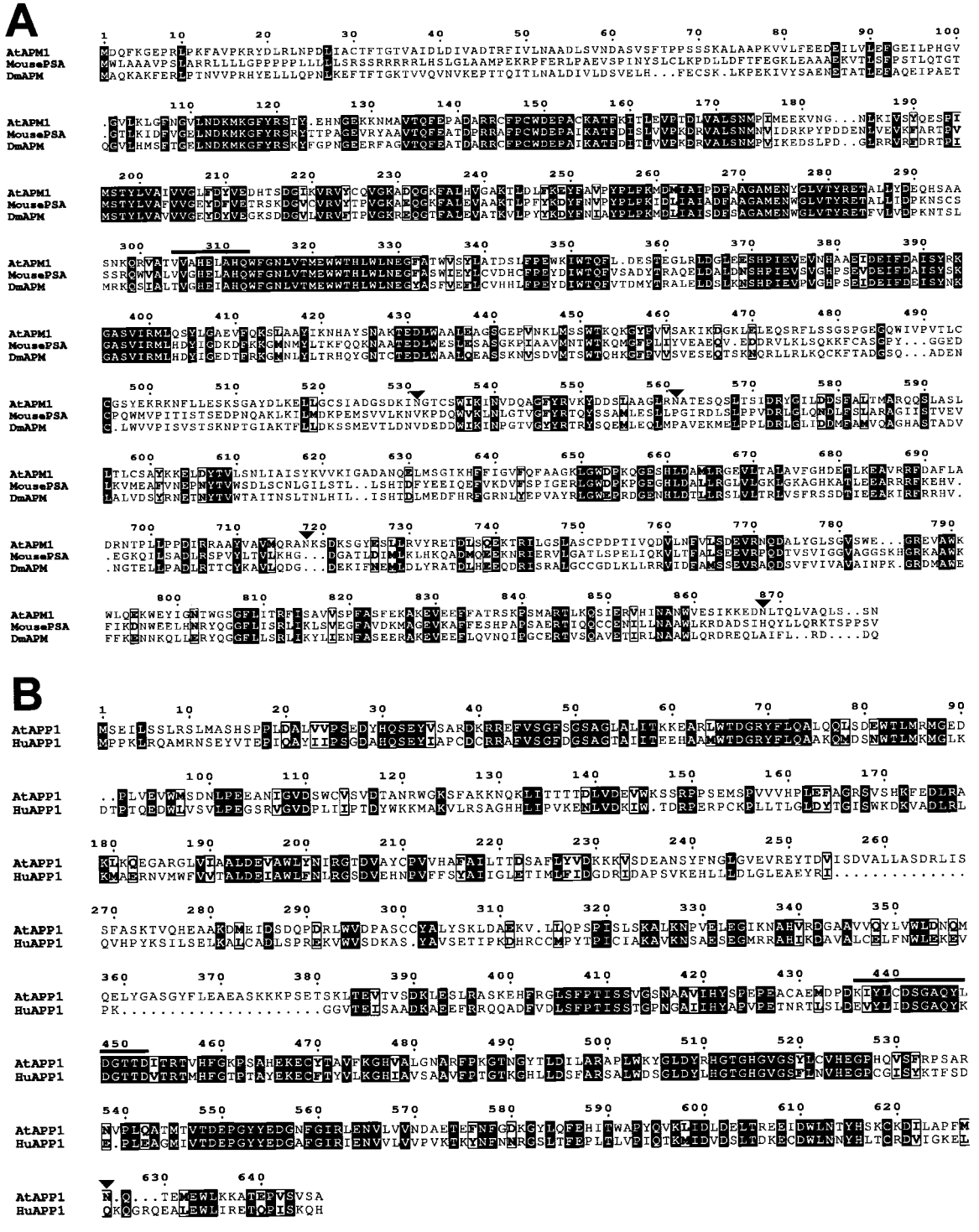

Figure 3. Multiple sequence alignments of AtAPM1 and AtAPP1 with orthologous animal proteins. Consensus sequences are shadowed in black; conserved sequences are in white boxes. Putatative catalytic sites are indicated by solid lines. Glycosylation sites are indicated by triangles. A, AtAPM1. Mouse PSA, Mouse puromycin-sensitive microsomal AP (Q11011); DmAPM, *Drosophila melanogaster* puromycin-sensitive AP (AAG48733). B, AtAPP1. HuAPP1, Human cytosolic APP1 (AAH05126). Human membrane-bound APP2 (AAG28480) used to determine consensus alignment is not shown.

light treatments, PCR of three Arabidopsis cDNA libraries, or examination of expressed sequence tag databases (data not shown). An alignment of the annotated sequence suggests that *AtAPP2* is a pseudogene. In light of these results, further analysis of *AtAPP2* expression was not pursued.

mRNA Expression of *AtAPM1* and *AtAPP1*

Previous histochemical studies showed that AP and NPA amidase activities were undetectable in seedlings until 3 d after germination, reached a peak at 5 d, and were present in all mature tissues, especially flowers, upper inflorescences, and growing regions of roots (Murphy and Taiz, 1999a, 1999b). Expression of both *AtAPM1* and *AtAPP1* at the mRNA level was consistent with the spatial and temporal patterns of histochemical data. As shown in Figure 4A, *AtAPP1* and *AtAPM1* were expressed in all of the adult tissues tested. *AtAPM1* mRNA was most abundant in young flowers, upper inflorescence stems, and rosette leaves. *AtAPM1* expression was roughly equal in roots, cauline leaves, lower inflorescence stems, and mature flowers. *AtAPM1* mRNA steady-state levels were very low in siliques and developing seeds. *AtAPP1* mRNA was most abundant in roots, mature flowers, and rosette leaves, all of which had steady-state mRNA levels at least twice those found in cauline leaves, lower inflorescence stems, upper inflorescence stems, and siliques. Steady-state mRNA levels in young flowers were barely detectable.

As shown in Figure 4B, *AtAPM1* expression began at 3 d and peaked at 5 d. *AtAPM1* expression levels remained constant from 7 to 10 d. *AtAPP1* expression from 2 to 10 d was similar to *AtAPM1* expression. Expression of *AtAPP1* began at 3 d, peaked at 5 d, then decreased to a basal level that remained constant through 10 d.

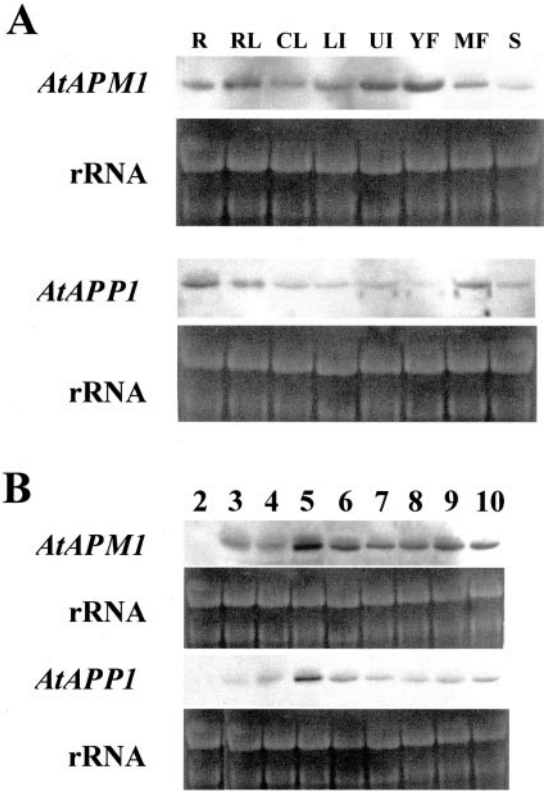

Figure 4. AtAPM1 and *AtAPP1* expression in adult and seedling tissue. A, Northern blots of adult tissue. Total RNA (7.26 μg) was extracted from roots (R), rosette leaves (RL), cauline leaves (CL), lower inflorescence stems (LI), upper inflorescence stems (UI), young flowers (YF), mature flowers (MF), and siliques (S). Blots were probed and visualized with digoxygenin (DIG)-labeled *AtAPM1* and *AtAPP1* probes. rRNA is shown as gel loading control. B, Northern-blot analysis of *AtAPM1* and *AtAPP1* mRNA in 2- to 10-d-old seedlings. Ten micrograms of total RNA was extracted and probed with DIG-labeled probes.

Immunochemical Localization of AtAPM1 and AtAPP1

Because PM APs of these two types had not been described before in plants, AtAPM1 and AtAPP1 were further identified by immunochemical means. Polyclonal antibodies to AtAPM1 and AtAPP1 were prepared (see "Materials and Methods") and used to assay the cellular partitioning of the native APs. As shown in Figure 5A, AtAPM1 was visible as a single protein with an apparent molecular mass of 103 kD in microsomal and PM (P5) fractions from 5-d-old seedlings. In addition to the 103-kD protein, 42- (doublet), and 38-kD proteins were detected in PM fractions from 5.5-d-old seedlings (P5.5). Higher levels of the 42-kD protein doublet were also found in cellular debris (Fig. 5A). A protein with an approximate molecular mass of 85 kD was detected in the soluble fraction. Although the 85-kD band may be a soluble protein encoded by a gene with regions of homology to *AtAPM1*, it is also consistent with proteolytic processing of AtAPM1 at the carboxy-terminal border of the conserved transmembrane domain to produce a soluble 85-kD product.

AtAPP1 was visible as a faint doublet with an approximate molecular mass of 71 kD in cellular debris and microsomal fractions, and was clearly evident in soluble fractions. The upper band coincides with the glycosylated form on PAS gels (Fig. 1C). A single 71-kD protein coinciding with the glycosylated form was detected in AtAPP1 western blots of PM fractions (PM1 and PM2), although the signal was much stronger in 5-d-old seedlings compared with 5.5-d-old seedlings. AtAPP1 was not detected in seedling PM fractions again until after 9 d (data not shown). The presence of a single AtAPP1 band in PM fractions is consistent with the prediction that the glycosylated form of AtAPP1 would be loosely associated with the PM and that the non-glycosylated form would be found in soluble fractions.

In microsomal preparations from mature tissues, the anti-AtAPM1 antibody strongly reacted with a 42-kD doublet in roots and leaves and faintly with a

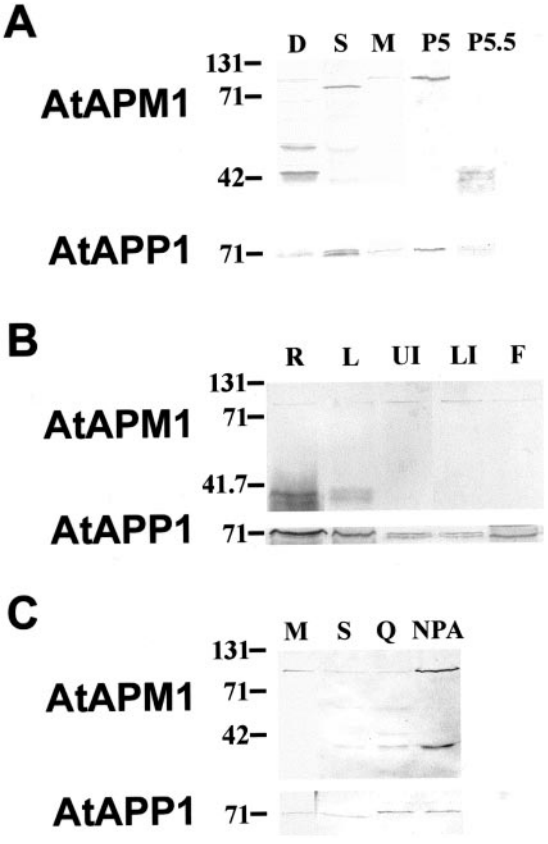

Figure 5. Immunolocalization of AtAPM1 and AtAPP1 in Arabidopsis. Western blots with polyclonal anti-AtAPM1 and AtAPP1 antibodies. In western blots utilizing the anti-AtAPP1 polyclonal antibodies, only protein bands that did not cross-react with pre-immune antisera are shown. A, Cellular partitioning of the native AtAPM1 and AtAPP1 proteins. Total protein (10 μg) from 5-d-old light-grown seedlings was used in all cases except lane P5.5, which used protein from 5.5-d-old seedlings. D, Cellular debris; S, soluble; M, microsomal; P5, PM proteins from 5-d-old seedlings; P5.5, PM proteins from 5.5-d-old seedlings. B, Microsomal preparations (10 μg of total protein) from adult tissues. R, Roots; L, rosette leaves; UI, upper inflorescence; LI, lower inflorescence; F, flowers. C, Western-blot analysis of Tyr-AP peak fractions from each purification stage with anti-AtAPM1 and AtAPP1 polyclonal antibodies. All samples are from 5-d-old light-grown Arabidopsis seedlings. Ten micrograms of total protein was used in lanes M, S, and Q. Two hundred nanograms of total protein was used in lane NPA. M, Microsomal; S, Sephacryl S-300; Q, Q anion-exchange; NPA, NPA affinity.

103-kD protein in inflorescences and flowers (Fig. 5B). Western blots with the anti-AtAPP1 antibody indicated that the highest levels of AtAPP1 are found in roots followed by leaves with somewhat higher levels in flowers than inflorescences.

The anti-AtAPP1 and anti-AtAPM1 antibodies were used to track the native AtAPP1 and AtAPM1 proteins throughout the steps of the same purification scheme that was initially used to isolate them (Fig. 1A). As shown in Figure 5C, the anti-AtAPM1 antibodies cross-reacted with a single protein with an apparent molecular mass of 103 kD in the microsomal fraction, but reacted with four proteins in the S-300 and Q-column fractions (103, 55, 42, and 38 kD). After NPA affinity purification, two distinct protein bands were detected at 103 and 42 kD, both of which corresponded to glycoproteins on PAS-stained gels (not shown). Incubation of an NPA affinity fraction blot with anti-AtAPM1 antibodies resulted in a signal approximately 5 times that of the preceding anion-exchange blot (Fig. 5C) despite a 50 times decrease in total protein loaded.

AtAPP1 was visible as a faint 71-kD doublet in microsomes and as a single 71-kD protein in S-300, Q-column, and NPA affinity fractions. Again, the NPA affinity fraction shown contains 50 times less total protein than the Q-resin anion-exchange lane.

AP Activity and Metal Binding of AtAPM1 and AtAPP1 Synthesized by in Vitro Translation

AtAPM1 and AtAPP1 proteins were synthesized in vitro from full-length cDNA (see "Materials and Methods"). APs were then purified by bestatin affinity chromatography and analyzed by SDS-PAGE (data not shown). A strong 103-kD band and weak 42-kD band were visible on gels from AtAPM1 reactions. A single 71-kD band was visible on gels from AtAPP1 reactions. No protein glycosylation was detected by PAS staining. Results from AP assays of AtAPM1 and AtAPP1 are shown in Table IV. Despite a lack of glycosylation, the substrate specificities were quite similar to those observed in NPA affinity Fraction II. Inhibition by EGTA is consistent with biochemical and histochemical evidence that AtAPM1 is a metallopeptidase and AtAPP1 is a metal-activated peptidase. However, the inhibition of both AP activities by the flavonoid kaempferol was less than expected from whole membrane studies

Table IV. *Enzymatic assays of AtAPM1 and AtAPP1 produced by in vitro translation*

AP and amidase assays with substrates and inhibitors indicated. Inhibitor concentrations used were as in Table II. Units are nmol AFC or β-NA released min^{-1} mg^{-1}. Values reported are means and SD of three independent experiments. Student-Newman-Keuls ANOVA indicates that the Tyr-AFC-related values reported are different from a normal distribution ($P < 0.001$). Values marked with an asterisk differ from controls in pair-wise comparisons ($P < 0.05$).

Substrate/Inhibitor	AtAPM1	AtAPP1
	nmol min^{-1} mg^{-1}	
Tyr-AFC	59 ± 5.8	36 ± 4.9
Tyr-AFC + kaempferol	32 ± 3.1*	30 ± 5.5
Tyr-AFC + PAQ22	17 ± 5.4*	47 ± 3.1*
Tyr-AFC + apstatin	54 ± 6.9	15 ± 4.7*
Tyr-AFC + EGTA	16 ± 6.4*	19 ± 2.2*
Ala-Pro-AFC	6 ± 4.2	74 ± 3.1
Ala-AFC	35 ± 4.2	5 ± 4.8
Pro-AFC	18 ± 5.3	29 ± 6.1
Trp-AFC	4 ± 3.2	20 ± 1.7
Leu-AFC	5 ± 3.1	7 ± 1.9
NPA	8 ± 3.4	3 ± 1.4

(Murphy and Taiz, 1999b). NPA was hydrolyzed at rates <50% of those in Fraction II. When assayed for AP activity, the pre-immune sera for both anti-AP antibodies had high levels of AP activity (not shown). As such, antibody inhibition of AP activity was not assayed.

Because microsomal APs in mammals are metalloenzymes and P-type APs are often metal activated, the APs purified from the in vitro system were incubated in buffered one-fourth-strength Murashige and Skoog growth media ± Brij35, washed, and then assayed for metal content by inductively coupled plasma-mass spectrometry (MS). AtAPM1 bound Zn: protein at a molar ratio of approximately 1:1 with no differences detected ± Brij 35. AtAPP1, however, bound both Mn and Zn in an approximately 1:1 ratio, but Mn represented approximately 15% with Brij35 present and approximately 98% without Brij35, suggesting that a hydrophobic environment may affect its specificity and activity.

[^{3}H] NPA-Binding Assays

To determine whether affinity for immobilized NPA reflects affinity for free NPA, dialyzed NPA affinity fractions were assayed for specific binding to [^{3}H] NPA. As shown in Table V, no specific [^{3}H] NPA binding was detected in peak fraction I. NPA affinity peak fractions II through IV exhibited increasing levels of specific NPA binding consistent with their NPA affinity elution profiles. After overnight incubation with a 1:500 (v/v) dilution of combined anti-AtAPM1 and anti-AtAPP1 polyclonal antibodies, combined fraction II- and III-specific NPA binding was reduced to <40% of controls (fraction II + III without antibodies). Specific NPA binding of in vitro AtAPM1 and AtAPP1 translation products was <35% of the NPA specific binding activity of affinity fractions II and III.

Table V. *Specific [^{3}H]NPA binding of PM vesicles, affinity fractions, and in vitro translation products of AtAPM1 and AtAPP1*

Specific activity is calculated as [^{3}H]NPA binding − [^{3}H]NPA binding in the presence of 1,000× cold NPA. Fractions I through IV, NPA affinity fractions I–IV; APAb, mixed polyclonal anti-AtAPM1 and AtAPP1 antibodies (see "Materials and Methods"); in vitro, in vitro translation products. Values reported are means and SD of three independent experiments. Student-Newman-Keuls ANOVA indicates that the values reported are different from a normal distribution ($P < 0.001$). Values with an asterisk differ from their control in pairwise Student's t tests ($P < 0.01$).

Sample	[^{3}H]NPA Bound
	pmol mg^{-1}
PM	0.1 ± 0.03
Fraction I	0.0 ± 0.03
Fraction II	7.1 ± 1.67
Fraction III	8.2 ± 1.25
Fraction IV	17.2 ± 3.07
Fraction II + III	17.8 ± 2.52
Fraction II + III + APAb	5.9 ± 3.55*
Fraction IV + APAb	16.8 ± 3.25
In vitro AtAPM1	3.2 ± 1.07
In vitro AtAPP1	1.9 ± 1.6

Purification of AP-Associated Proteins Displaced by NPA

The Tyr-AP peak fraction after anion-exchange chromatography showed one band of an apparent molecular mass of 35 kD (p35) and another diffuse band at 28 to 30 kD (p29) on SDS gels. Proteins could not be detected on silver-stained SDS-PAGE gels after further purification by NPA chromatography (not shown). A precipitate that formed during the initial incubation step of NPA affinity chromatography was collected, partially solubilized in SDS, and analyzed by SDS-PAGE. The two protein bands previously noted plus another faint band with an apparent molecular mass of 46 kD (p46) were visible. All three bands were identified as glycoproteins by PAS staining (not shown).

Amino acid sequences of fragments of p29 and p30 proteins were determined as described above. The fragment from the p35, (K) PTLPSPVYTPPVY, identified p35 as AtPRP3 (GenBank accession no. AAF64550), the gene product of a gene recently localized to the precise regions in Arabidopsis roots and the root-shoot transition zone stained by NPA (Murphy and Taiz, 1999a; Bernhardt and Tierney, 2000). p29 appeared to contain a mixture of at least two PRPs because the mixed sequence obtained, (K) I/TPN/HAFSGLRVTID/E, is found in at least two previously identified PRPs (GenBank accession nos. AAF64550 and AAF64551). Because the protein entered in GenBank as AAF64551 is predicted to be 45 kD, the 46-kD band was not sequenced.

DISCUSSION

We have described herein the identification of two novel APs highly homologous with mammalian and fungal PM APs involved in peptide hormone processing, receptor activation, processing of secreted proteins, and extracellular matrix interactions. Because no other APs of this type have been previously identified in plants, their role in growth, development, and signaling can, at this point, only be inferred from the activities of orthologous proteins in animals, the association of PM APs with regions of differentiation and auxin-induced growth, and the evidence that common AP substrates and inhibitors have NPA-like effects on growth (Murphy and Taiz, 1999a, 1999b; Murphy et al., 2000). The sequence homology of AtAPM1 with the mammalian IRAP, which plays an essential role in vesicular cycling of the GLUT4 transporter (Baumann and Saltiel, 2001), suggests a similar role in the asymmetric distribution of plant transport proteins. In planta localization and loss-of-function studies combined with complemen-

tation studies in *Saccharomyces cerevisiae* now underway will examine the connection between AP activity and NPA-sensitive auxin transport inhibition.

Both of the APs bind NPA with lower affinity than the multiple drug resistance-type *p*-glycoproteins. However, because low-affinity NPA binding appears to correlate with auxin transport inhibition at least as well as high-affinity binding (Michalke et al., 1992), the weaker affinity of PM APs for NPA does not rule out a role in auxin transport. In mammals, PM APs are closely associated in functional complexes (Medeiros and Turner, 1994). The presence of copurifying membrane surface proteins and the synergistic effects on AP activity found when high- and low-affinity NPA-binding fractions were reconstituted suggests that the APs identified function as components of protein complexes. The presence of cell surface proteins in NPA-binding fractions also suggests that NPA inhibition of auxin transport in intact tissues might involve more complex processes than those suggested by NPA binding to membrane vesicles alone.

The low levels of specific NPA-binding activity found with purified in vitro translation products of *AtAPM1* and *AtAPP1* may be indicative of a requirement for interactions with AP-associated proteins for efficient NPA binding. On the other hand, the in vitro translation products were not glycosylated. Glycosylation of the native proteins may be required for efficient binding and enzymatic activity because treatment of affinity fraction II with deglycosylating enzymes dramatically decreased specific NPA binding (A.S. Murphy, unpublished data).

NPA amidase and Ala-AP activity in affinity fraction III appear to correlate with levels of a truncated form AtAPM1 (AtAPM1Δ) and two novel AP-associated proteins, AtMyA1, a paralog of *B. napus* myrosinase-associated proteins with Jacalin lectin and Kelch repeat domains, and AtAPL1, a protein with weak homology to anther-specific PRPs. It must still be determined whether purified AtMya1 or AtAPL1 possess amidase activity, as is suggested by hydrolase motifs in their predicted sequences, or whether they act synergistically to promote the activity of AtAPP1 and AtAPM1.

The association of AtGSTF2 with AP-associated proteins is not surprising because its interaction with NPA has been documented before (Zettl et al., 1994). Localization and expression studies of AtGSTF2 indicate that its expression is induced by auxin accumulation, that it colocalizes with regions of NPA staining, and that its expression is enhanced under the same conditions that enhance AP activity (A.S. Murphy and P.B. Goldsbrough, unpublished data).

Flavonoid binding with APs and higher affinity NPA-binding proteins is also consistent with previous findings. Aglycone flavonoids have been shown to modulate auxin transport and compete with NPA binding to microsomal vesicles (Jacobs and Rubery, 1988; Faulkner and Rubery, 1992; Bernasconi, 1996; Murphy et al., 2000; Brown et al., 2001). Flavonoid inhibition of PM AP activity has been demonstrated in Arabidopsis (Murphy and Taiz, 1999b) and is well documented in studies of multidrug resistance-type *p*-glycoproteins in other species (Castro and Altenberg, 1997). Weak flavonoid binding to AtGSTF2 has also recently been demonstrated (A.S. Murphy and P.B. Goldsbrough, unpublished data). A model of multiple flavonoid-binding sites of varied affinity is also consistent with previous biochemical studies in Arabidopsis. Murphy et al. (2000) found that flavonoid displacement of NPA binding to Arabidopsis microsomal vesicles was nearly linear for most of the concentration range assayed, but also found that two distinct phases were evident in the lowest and highest concentration ranges, suggesting multiple binding sites or cooperative binding.

The evidence that cell wall PRPs that play a crucial role in seedling growth and development (Bernhardt and Tierney, 2000) are displaced from PM-associated AP fractions by NPA suggests that they may be endogenous substrates of one or both APs and that NPA may interfere with that interaction in vivo. It is also unclear whether the GPI-anchored arabinogalactan protein AtFAGP2 or the PRP AtAPL1 are substrates of the PM APs as well as components of the PM AP protein complex. PMAPs may have an additional role in processing of proteins in the endomembrane system of mature plants, as microsomal protein levels derived from mature plant tissues were much higher than in seedlings (Fig. 5B) and no AtPP1 or AtAPPM1 proteins were detected in isolated chloroplasts or vacuolar vesicles (A.S. Murphy, unpublished results).

The universality of these results is still to be determined. NPA-hydrolyzing protein complexes may only be present in less NPA-sensitive species like cucurbits, crucifers, legumes, and maize (*Zea mays*) and not in NPA-sensitive species like tomato (*Lycopersicon esculentum*), beet (*Beta vulgaris*), spinach (*Spinacia oleracea*), and lettuce (*Lactuca sativa*). Similarly, localization patterns of NPA hydrolysis vary among species (A.S. Murphy, unpublished data), and some AP-associated proteins, like AtMyA1, an ortholog of proteins copurifying with glucosinolate-processing enzymes (Taipalensuu et al., 1997), are unlikely to be present in non-cruciferous species. However, because these two PM-associated APs are so highly conserved across the animal, fungi, and plant kingdoms, their function in the model plant Arabidopsis is likely to extend, at least partially, to other plant species.

MATERIALS AND METHODS

Plant Material, Growth Conditions, and Reagents

All plant tissues for biochemical assays were derived from the Wassilewskija ecotype of Arabidopsis. For cloning of the AP genes, DNA and RNA were obtained from the

Columbia ecotype of Arabidopsis. Seeds of both ecotypes were obtained from the Arabidopsis Biological Resource Center (Ohio State University, Columbus). Unless otherwise noted, seedlings were grown in the vertical mesh transfer apparatus (Murphy and Taiz, 1995) under continuous light. Mature plants were grown in soil in 16-h days under greenhouse conditions.

Unless otherwise noted, all reagents were obtained from Sigma (St. Louis). PAQ-22 was a gift from Dr. Yuichi Hashimoto (Institute of Molecular and Cellular Biosciences, University of Tokyo). [^{3}H] NPA was a gift from Novartis Crop Protection Systems (Research Triangle, NC). All buffers were made fresh on the day of use with the exception of PM phase buffers, which were made up without reductants and protease inhibitors 1 week in advance, stored at 4°C, and then used immediately after the addition of inhibitors and reductants. Anti-BIP polyclonal antibodies used in assessments of PM vesicle purity were donated by Dr. Maarten Chrispeels (Biology Department, University of California, San Diego).

Enzyme and Binding Assays

Enzymatic cleavage of NPA and AP substrates was assayed as described previously (Murphy and Taiz, 1999a, 1999b) with the exception that enzymatic activity was assayed in a buffer consisting of 20 mM BisTris propane-MES [2-(*N*-morpholino)-ethanesulfonic acid] (pH 6.5), 0.05% (w/v) Brij-35, 5% (w/v) glycerol, 10 μM MnCl2, 5 μM ZnCl2, and 50 μM $CaCl_2$. Enzymatic cleavage was assayed using either an LS-5 (Perkin-Elmer Instruments, Shelton, CT), LS-50B (Perkin-Elmer Instruments), or Spectramax GeminiXS fluorometric spectrophotometer (Molecular Devices, Sunnyvale, CA) under saturating conditions at room temperature with 10 μM amidomethylcoumarin (AMC), 20 μM AFC, or 50 μM naphthtylamide amino acyl-substrates as noted. For assays using Gly-Pro AMC, the AP Assay buffer was brought to a pH of 7.5 with KOH. PMSF was used at 50 μM where indicated. Optimal inhibitor concentrations were determined as described previously (Murphy and Taiz, 1999a, 1999b). AP activity was visualized after nondenaturing PAGE utilizing Tyr-AFC or Tyr-AFC-impregnated enzyme overlay membranes (Enzyme Systems, Livermore, CA) according to the manufacturer's protocol.

NPA-binding assays were performed as described previously (Murphy et al., 2000). For assays of antibody interference with NPA binding, samples were pre-incubated overnight at 4°C in assay buffer with 1:500 (v/v) dilutions of polyclonal antibodies indicated, then assayed for NPA binding as described. Blanks for antibody interference assays were polyclonal antibodies alone. Flavonoid-binding assays were performed by incubating NPA affinity fractions with 10 μM each quercetin + kaempferol in 10 mM HEPES [4-(2-hydroxyethyl)-1-piperazineethanesulfonic acid] and 0.1% (w/v) Brij 35 (pH 6.5) for 30 min at 4°C. Fractions were then loaded into Microcon 3 spin filters (Amicon, Beverly, MA) and washed five times with 500 μL of buffer minus flavonoids. Retentates were then assayed spectrofluorometrically for flavonoid content using DPBA as described previously (Murphy et al., 2000; Peer et al., 2001).

Purification of PM APs

Microsomal preparations of 5-d-old Arabidopsis seedlings were prepared and assayed for purity as described previously (Murphy and Taiz, 1999a) with the exception that 500 μM benzamide and 500 μM benzamidine were added to the original homogenization buffer. Where indicated, PM-enriched fractions were also prepared by phase separation of microsomes as previously described. Prepared membranes were stored in liquid nitrogen. AP assays utilized Tyr-AMC unless otherwise noted. Membrane proteins were detergent solubilized by incubation with gentle shaking at 4°C for 30 min in a buffer consisting of 0.1% (w/v) Brij 35, 0.05% (w/v) CHAPS {3-[(3-cholamidopropyl)dimethylammonio]-1-propanesulfonic acid}, 10 mM BisTris propane-MES (pH 7.8), 250 mM Suc, 20% (w/v) glycerol, and 1 mM DTT followed by centrifugation at 100,000*g* for 30 min. All subsequent purification steps were performed at 7°C unless otherwise noted and fractions were stored at −70°C. The supernatant was applied to a 72 × 1 cm Sephacryl S-300 column (Pharmacia Biotech, Piscataway, NJ) that had been precalibrated with molecular mass standards (apoferritin, 443,000 D; urease, 240,000 D; β-amylase, 200,000 D; alcohol dehydrogenase, 150,000 D; bovine serum albumin, 66,000 D; glyceraldehydes dehydrogenase, 36,000 D; and trypsin inhibitor, 20,000 D) and eluted utilizing a running buffer (RB) containing 5% (w/v) glycerol, 0.1% (w/v) Triton X-100, 20 mM HEPES, pH 7.0, 100 μM DTT, 100 ng mL^{-1} leupeptin, 500 μM benzamide, and 500 μM benzamidine plus 100 mM KCl at a temperature of 7°C. Fractions (2 mL) were collected and assayed for total protein and Tyr-AP activity. Fractions with Tyr-AP activity were pooled as described (see "Results"), dialyzed at 4°C against 1 mM DTT, applied to a 5-mL Q-resin anion-exchange column (Bio-Rad, Hercules, CA), and eluted with a 0 to 350 mM KCl gradient in RB with HEPES replaced by Bis-Tris propane-MES. Fractions (1 mL) with Tyr-AP activity were retained and dialyzed against 1 mM DTT.

NPA was immobilized on amine-terminated magnetic beads (Sigma) utilizing the manufacturer's protocol with the exception that NPA was used in 5× molar excess to prevent nonamide coupling. The pH of buffers was maintained above pH 6.5 to prevent NPA hydrolysis, and coupling reactions were conducted at 1°C for 24 h. Coupled beads were washed extensively and stored at 4°C, pH 7.4. Fractions retained from anion-exchange chromatography were brought to pH 7.4 with BisTris propane-MES, mixed with NPA-conjugated magnetic beads, incubated at 4°C for 2 h with gentle shaking, then collected with a magnet. The beads were washed three times for 10 min at 4°C with RB (pH 7.4) minus protease inhibitors and containing 50 mM KCl. Fractions were then eluted in a 25 mM step gradient beginning at 100 mM and ending at 500 mM. Eluted fractions were dialyzed against RB + 50 mM KCl and then assayed for Tyr-AP activity. For reconstitution experi-

ments, different step gradient elutions were combined in equal portions and then dialyzed before AP assays.

GPI-anchored proteins were detected by Triton X-114 partitioning and phospholipase C enzymatic cleavage (Sherrier et al., 1999) followed by visualization on silver-stained two-dimensional gels. Western blots were generated as previously described (Murphy et al., 1997).

Electrophoresis and Amino Acid Sequencing of Purified Proteins

Native PAGE of AP complexes was performed according to the method of von Jagow and Schagger (1994). Proteins purified in the scheme above were separated by SDS-PAGE and visualized by Coomassie Blue or silver staining. Glycoproteins were detected by periodic acid Schiff's reagent staining (Leach et al., 1980) and enzymatic deglycosylation utilizing a Protein Deglycosylation Kit (Bio-Rad) according to the manufacturer's protocols. AtFAGP2 required chemical deglycosylation for sequencing (Schultz et al., 2000). For sequencing, fractions were separated by two-dimensional gel electrophoresis. Coomassie Blue-stained spots were cut out of gels, digested with trypsin, and separated by reverse-phase C18 HPLC. Amino acid sequences of fractions from selected peaks were then analyzed by Edman degradation as described previously (Murphy, et al., 1997). Molecular masses were confirmed in some cases by matrix-assisted laser desorption/ionization-time of flight-MS. In cases where insufficient amounts of protein could be obtained for amino acid sequencing, NPA affinity fractions eluted in the same KCl concentration steps from five purifications were pooled and separated by reverse-phase C8 HPLC. Fractions corresponding to A_{280} peaks were digested with trypsin and separated by reverse-phase C18 HPLC. Peak profiles were compared with those from blank trypsin digests. Fractions corresponding to major peaks not found in blanks were blotted to polyvinylidene difluoride membranes and sequenced. Sequences were compared with Arabidopsis genomic, cDNA, and predicted protein databases for unique matches. In cases where more than one sequence match of similar predicted molecular mass was obtained, additional fragments were sequenced until a unique match was identified.

Secondary structure, cellular localization, and posttranslational modification predictions were made utilizing RPS BLAST (NCBI), PSORT (http://psort.nibb.ac.jp/), PROSITE SCAN (http://npsa-pbil.ibcp.fr/cgi-bin/npsa_automat.pl?page=npsa_prosite.html), SOSUI membrane helix prediction (http://sosui.proteome.bio.tuat.ac.jp/sosuiframe0.html), and Big-PI GPI Predictor (http://mendel.imp.univie.ac.at/gpi/; Eisenhaber et al., 1998). Multiple sequence alignments were prepared with Multalin (Corpet, 1988).

Genomic DNA Analysis

Genomic DNA was extracted from 7-d-old Arabidopsis (Columbia) seedlings utilizing the DNAeasy kit (QIAGEN, Valencia, CA), digested with restriction enzymes as noted, and analyzed by Southern hybridization utilizing full-length cDNA probes labeled with the DIG Genius I DNA labeling and detection kit according to the manufacturer's protocols (Roche Molecular Biochemicals, Indianapolis). Both chemiluminescent and colorometric detection were used. Verified nucleotide sequences of *AtAPM1* and *AtAPP*1 had previously been obtained by comparison of RT-PCR products of 5-d-old seedling mRNA and published genomic sequences in the NCBI database. In all cases where a cDNA sequence diverged from the genomic consensus sequence, alternate cDNA sequences were obtained and inserted by restriction digest and ligation to produce the correct cDNA construct. The cDNA sequences for *AtAPP1* and *AtAPM1* were inserted into pGEM5zf plasmids and nucleotide sequences were confirmed by nucleotide sequencing on an ABI 310 automated sequencer (Applied Biosystems, Foster City, CA).

RNA Expression Studies

DIG-labeled DNA probes were produced using the Roche DIG PCR labeling kit according to the manufacturer's protocols (Roche Molecular Biochemicals). Primers used for *AtAPM1* probes (gttctcctggggaaggacaa and ttagtttgaagagagctgagcaacg) amplified a labeled product of 1,247 nucleotides (nucleotides 1,390–2,637 of the cDNA sequence). Primers used for *AtAPP1* probes (cctctaaaactgtccaaca and tcaagcggatacacttacaggtt) amplified a labeled product of 1,158 nucleotides (nucleotides 777–1935 of the cDNA sequence).

To assure that equal quantities of DIG-labeled probes were utilized in all experiments, probes were purified with Microcon 100 spin columns (Amicon), quantitated spectrophotometrically, and diluted to equal concentrations. Effectiveness of probes was then tested by Southern blotting of plasmids according to the manufacturer's protocols (Roche Molecular Biochemicals). Visualization of RNA expression with northern blots was conducted as described previously (Garcia-Hernandez et al., 1998).

Construction of Protein Expression Vectors

Full-length cDNA sequences of *AtAPM1* and *AtAPP1* without stop codons were inserted into the pFLAG carboxy terminal cytoplasmic expression plasmid (Sigma) utilizing *Sma*I and *Eco*RI restriction enzyme sites engineered into the 5′ ends of *AtAPM1* and *AtAPP1*, respectively, and a *Bgl*II site engineered into the 3′ end of both cDNA inserts. Sequences were verified by nucleotide sequencing and AP-FLAG fusion proteins were expressed in the BL21 pLysE expression strain of *Escherichia coli* (Invitrogen, San Diego). Because expression of *AtAPM1* proved to be toxic to bacteria, a truncated form of *AtAPM1* was prepared by excision of 835 nucleotides from the 5′ region of the *AtAPM1* cDNA by digestion of the pFLAGATAPM1 plasmid with *Bam*HI and subsequent religation to produce pFLAGAtAPM1Δ278. This resulted in the production of a truncated fusion protein lacking the

amino-terminal 278 amino acids, but still containing the putative catalytic site and carboxy-terminal extracellular domains. Bacteria expressing the truncated protein grew sufficiently to allow for recovery of the recombinant protein.

Expressed fusion proteins were solubilized in 8 M urea (AtAPM1Δ278FLAG) or 1% (w/v) SDS (AtAPP1FLAG) and identified by western blotting as described previously (Murphy et al., 1997) with an anti-FLAG M2 monoclonal antibody (Sigma). Fusion proteins were electroeluted, pooled, and dialyzed. Polyclonal antibodies were prepared by Covance Antibody Products in New Zealand White rabbits by standard methods (two for each fusion protein). Antibodies were purified from sera as described by Harlow and Lane (1988). The dialyzed antibody-containing pellet was resuspended in 2 mL of phosphate-buffered saline, and stored at 4°C until use. Antibodies were tested for reacitivity and specificity by ELISA and western blotting utilizing both expressed fusion proteins and native extracts of purified APs.

In Vitro Translation of AtAPP1 and AtAPM1

AtAPM1 and AtAPM1 proteins were produced in vitro with the TnT wheat germ extract system (Promega, Madison, WI) with the addition of 0.1% (w/v) Brij 35 to stabilize the synthesized proteins. AP proteins were purified using bestatin affinity chromatography. Bestatin was immobilized on an aminohexanoic acid Sepharose 4B column per the manufacturer's instructions (Sigma).

Metal-Binding Assays

In vitro-translated proteins were incubated in one-fourth-strength Murashige and Skoog medium; 10 mM HEPES, pH 6.5, 0.1% (w/v) Brij35 overnight at 4°C, then washed on Microcon 3 spin filters (Amicon) with 10 mM HEPES, pH 6.5. Protein samples were than assayed for metal content using a VGPQ ExCell inductively coupled plasma-MS (Thermo Elemental, Franklin, MA) at the Purdue-National Science Foundation Ionomics Analytical Facility.

ACKNOWLEDGMENTS

We would like to thank Drs. Mathias Müller and Paul Bernasconi for their advice on protein purification and characterization, Brett Lahner for performing metal assays, and Drs. Mark Jacobs, Gloria Muday, and Avtar Handa for their critical reading of the manuscript.

Received June 14, 2001; returned for revision July 22, 2001; accepted August 29, 2001.

LITERATURE CITED

Akasaki K, Yoshimoto H, Nakamura A, Shiomi H, Tsuji H (1995) Purification and characterization of a major kyotorphin hydrolyzing peptidase of rat brain. J Biochem **117:** 897–902

Baumann C, Saltiel A (2001) Spatial compartmentation of signal transduction in insulin action. BioEssays **23:** 215–222

Bernasconi P (1996) Effects of synthetic and natural protein Tyr kinase inhibitors on auxin efflux in zucchini (*Cucurbita pepo*) hypocotyls. Physiol Plant **96:** 205–210

Bernhardt C, Tierney M (2000) Expression of AtPRP3, a Pro-rich structural cell wall protein from Arabidopsis, is regulated by cell-type-specific developmental pathways involved in root hair formation. Plant Physiol **122:** 705–714

Brown DE, Rashotte AM, Murphy AS, Normanly J, Tague BW, Peer WA, Taiz L, Muday GK (2001) Flavonoids act as negative regulators of auxin transport in vivo in Arabidopsis. Plant Physiol **126:** 524–535

Castro AF, Altenberg GA (1997) Inhibition of drug transport by genistein in multidrug-resistant cells expressing *p*-glycoprotein. Biochem Pharmacol **53:** 89–93

Chen R, Hilson P, Sedbrook J, Rosen E, Caspar T, Masson PH (1998) The *Arabidopsis thaliana* AGRAVITROPIC 1 gene encodes a component of the polar-auxin-transport efflux carrier. Proc Natl Acad Sci USA **95:** 15112–15117

Corpet F (1988) Multiple sequence alignment with hierarchical clustering. Nucleic Acids Res **16:** 10881–10890

Dean MF, Sansom P (2000) Link peptide cartilage growth factor is degraded by membrane proteinases. Biochem J **349:** 473–479

Diaz E, Schimmoller F, Pfeffer SR (1997) A novel Rab9 effector required for endosome to TGN transport. J Cell Biol **138:** 283–290

Eisenhaber B, Bork P, Eisenhaber F (1998) Sequence properties of GPI-anchored proteins near the omega-site: constraints for the polypeptide binding site of the putative transamidase. Protein Eng **11:** 1155–1161

Faulkner IJ, Rubery PH (1992) Flavonoids and flavonoid sulphates as probes of auxin-transport regulation in *Cucurbita pepo* hypocotyl segments and vesicles. Planta **186:** 618–625

Foulon T, Cadel S, Cohen P (1999) Aminopeptidase B (EC 3.4.11.6). Int J Biochem Cell Biol **31:** 747–750

Gälweiler L, Guan C, Mueller A, Wisman E, Mendgen K, Yephremov A, Palme K (1998) Regulation of polar auxin transport by AtPIN1 in *Arabidopsis* vascular tissue. Science **282:** 2226–2230

Garcia-Hernandez M, Murphy A, Taiz L (1998) Metallothioneins 1 and 2 have distinct but overlapping expression patternsin Arabidopsis. Plant Physiol **118:** 387–397

Geissler AE, Pilet PE, Katekar GF (1985) Growth and gravireaction of maize roots treated with a phytotropin. J Plant Physiol **119:** 25–34

Harlow I, Lane D (1988) Antibodies: a laboratory manual. Cold Spring Harbor Press, Cold Spring Harbor, NY

Jacobs M, Rubery P (1988) Naturally occurring auxin transport regulators. Science **241:** 346–349

Jensen PJ, Hangarter RP, Estelle M (1998) Auxin transport is required for hypocotyl elongation in light-grown but not dark-grown Arabidopsis. Plant Physiol **116:** 455–462

Jouannic N, Lepetit M, Vergnolle C, Cantrel C, Gardies AM, Kader JC, Arondel V (1998) Isolation of a cDNA from *Arabidopsis thaliana* that complements the *sec14* mutant of yeast. Eur J Biochem **258:** 402–410

Kang BH, Busse JS, Dickey C, Rancour DM, Bednarek SY (2001) The Arabidopsis cell-plate associated dynamin-like protein, ADL1Ap, is required for multiple stages of plant growth and development. Plant Physiol **126:** 47–68

Katekar GF, Geissler AE (1989) The distribution of the receptor for 1-N-naphthylphthalamic acid in different tissues of maize. Physiol Plant **76:** 183–186

Katekar GF, Geissler AE, Kennard CHL, Smith G (1987) Recognition of phytotropins by the receptor for 1-N-napththylphthalamic acid. Phytochemistry **26:** 1257–1267

Komoda M, Kakuta H, Takahashi H, Fujimoto Y, Kadoya S, Kato F, Hashimoto Y (2001) Specific inhibitor of puromycin-sensitive aminopeptidase with a homophthalimide skeleton: identification of the target molecule and a structure-activity relationship study. Bioorg Med Chem **9:** 121–131

Leach BS, Collawn JF, Fish WW (1980) Behavior of glycopolypeptides with empirical molecular weight estimation methods. Biochemistry **19:** 5734–6747

Lomax TL, Muday GK, Rubery PH (1995) Auxin transport. *In* PJ Davies, ed, Plant Hormones: Physiology, Biochemistry and Molecular Biology, Ed 2. Kluwer, Dordrecht, The Netherlands, pp 509–530

Luschnig L, Gaxiola RA, Grisafi P, Fink GR (1998) EIR1, a root specific protein involved in auxin transport, is required for gravitropism in *Arabidopsis thaliana*. Genes Dev **12:** 2175–2187

Medeiros MDS, Turner AJ (1994) Processing and metabolism of peptide-YY: pivotal roles of dipeptidyl peptidase-IV, aminopeptidase P, and endopeptidase-24.11. Endocrinology **134:** 2088–2094

Michalke W, Katekar GF, Geissler AE (1992) Phytotropin-binding sites and auxin transport in *Cucurbita pepo*: evidence for two recognition sites. Planta **187:** 254–260

Muday GK (2001) Maintenance of asymmetric cellular localization of an auxin transport protein through interaction with the actin cytoskeleton. J Plant Growth Regul **19:** 385–396

Müller A, Guan C, Gälweiler L, Taenzler P, Huijser P, Marchant A, Parry G, Bennett M, Wisman E, Palme K (1998) AtPIN2 defines a locus of *Arabidopsis* for root gravitropism control. EMBO **17:** 6903–6911

Murphy A, Peer WA, Taiz L (2000) Regulation of auxin transport by aminopeptidases and endogenous flavonoids. Planta **211:** 315–324

Murphy A, Taiz L (1995) A new vertical mesh transfer technique for metal-tolerance studies in Arabidopsis: ecotype variation and copper-sensitive mutants. Plant Physiol **108:** 29–38

Murphy A, Taiz L (1999a) Localization and characterization of soluble and plasma membrane aminopeptidase activities in Arabidopsis seedlings. Plant Physiol Biochem **37:** 431–443

Murphy A, Taiz L (1999b) Naphthylphthalamic acid is enzymatically hydrolyzed at the hypocotyl-root transition zone and other tissues of *Arabidopsis thaliana* seedlings. Plant Physiol Biochem **37:** 413–430

Murphy A, Zhou J Goldsbrough PB, Taiz L (1997) Purification and immunological identification of metallothioneins 1 and 2 from *Arabidopsis thaliana*. Plant Physiol **113:** 1293–1301

Nissen JB, Iversen L, Kragballe K (1995) Characterization of the aminopeptidase activity of epidermal leukotriene A_4 hydrolase against the opioid dynorphin fragment 1–7. Br J Dermatol **133:** 742–749

Noh B, Murphy AS, Spalding EP (2001) *Multidrug Resistance*-like genes of Arabidopsis required for auxin transport and auxin-mediated development. Plant Cell **13:** 2441–2454

Peer WA, Brown D, Taigue BW, Muday GK, Taiz L, Murphy AS (2001) Flavonoid accumulation patterns of transparent testa mutants of *Arabidopsis*. Plant Physiol **126:** 536–548

Ponomarev E, Tarasenko TN, Sapozhnikov AM (2000) Splenic cytotoxic cells recognize surface Hsp70 on culture adapted EL-4 mouse lymphoma cells. **74:** 133–139

Prime TA, Sherrier DJ, Mahon P, Packman LC, Dupree P (2000) A proteomic analysis of organelles from *Arabidopsis thaliana*. Electrophoresis **21:** 3488–3499

Rubery PH (1990) Phytotropins: Receptors and endogenous ligands. Soc Exp Biol **44:** 119–146

Sankarnarayan R, Sekar K, Banerjee R, Sharma V, Surolia A, Vijayan M (1996) A novel mode of carbohydrate recognition in jacalin, a Moraceae plant lectin with a beta-prism fold. Nat Struct Biol **3:** 596–603

Santos AN, Langner J, Herrmann M, Riemann D (2000) Aminopeptidase N/CD13 is directly linked to signal transduction pathways in monocytes. Cell Immunol **201:** 22–32

Schultz CJ, Johnson KL, Currie G, Bacic A (2000) The classical arabinogalactan protein family of Arabidopsis. Plant Cell **12:** 1751–1767

Sherrier DJ, Prime TA, Dupree P (1999) Glycosylphopsphatidylinositol-anchored cell-surface proteins from Arabidopsis. Electrophoresis **20:** 2027–2035

Sidler M, Hassa P, Hasan S, Ringli C, Dudler R (1998) Involvement of an ABC transporter in a developmental pathway regulating hypocotyl cell elongation in the light. Plant Cell **10:** 1623–1636

Taipalensuu J, Eriksson S, Rask L (1997) The myrosinase-binding protein from *Brassica napus* seeds possesses lectin activity and has a highly similar vegetatively expressed wound-inducible counterpart. Eur J Biochem **250:** 680–688

Taylor A (1996) Aminopeptidases: occurrence, regulation, and nomenclature. *In* A Taylor, ed, Aminopeptidases. R.G. Landes, Georgetown, TX, pp 1–20

Utsuno K, Shikanai T, Yamada Y, Hashimoto T (1998) AGR, an AGRAVITROPIC locus of *Arabidopsis thaliania*, encodes a novel membrane protein family member. Plant Cell Physiol **39:** 1111–1118

Venema RC, Ju H, Zou R, Venema VJ, Ryan JW (1997) Cloning and tissue distribution of human membrane-

bound aminopeptidase P. Biochim Biophys Acta **1354:** 45–48

von Jagow G, Schagger H (1994) A Practical Guide to Membrane Protein Purification. Academic Press, San Diego, CA

Walling L, Gu YQ (1996) Plant aminopeptidases. *In* A Taylor, ed, Aminopeptidases. R.G. Landes, Georgetown, TX, pp 173–218

Zettl R, Schell J, Palme K (1994) Photoaffinity labeling of *Arabidopsis thaliana* plasma membrane vesicles by 5-azido-(7–3H) indole-3-acetic acid: identification of a glutathione S-transferase. Proc Nat Acad Sci USA **91:** 689–693

Zhao L, Gregoire F, Sui HS (2000) Transient induction of ENC-1, a kelch-related actin binding protein, is required for adipocyte differentiation. J Biol Chem **275:** 16845–16850